NOTE
DE CENTRE

N° 32

A subgrid convection scheme for representing dry, moist and precipitating convection in large-scale models, PCMT. Part 1: equations

Jean-Marcel Piriou, Jean-François Guérémy and Yves Bouteloup

Novembre 2018

CENTRE NATIONAL
DE RECHERCHES MÉTÉOROLOGIQUES

A subgrid convection scheme for representing dry, moist and precipitating convection in large-scale models, PCMT. Part 1: equations

Jean-Marcel Piriou, Jean-François Guérémy and Yves Bouteloup*

CNRM-GAME, Meteo-France-CNRS UMR 3589

*Correspondence to: CNRM-GAME, Meteo-France-CNRS UMR 3589, 42 av. Coriolis, F-31057 Toulouse Cedex. E-mail: jean-marcel.piriou@meteo.fr, jean-francois.gueremy@meteo.fr, yves.bouteloup@meteo.fr

A convection scheme is presented, PCMT for Prognostic Condensates Microphysics and Transport, that handles convective condensated species (liquid, ice, rain and snow) prognostically, as well as vertical velocity. A symmetric and conservative equation set is developed to predict in-cloud and environmental water species and their entrainment - detrainment processes. Grid-scale budget equations separate microphysics and transport terms, thus becoming closer to those of convection-resolving-models (CRMs) or large-eddy simulations (LES), making possible detailed validations of parameterized cloud budgets versus CRMs, even in transitory states.

The prognostic microphysics is called twice: inside sub-grid-scale convective updraft and in the resolved-scale environment. In such a convection scheme, a large part of convective precipitation occurs from condensates detrained in the environment near cloud top, forming anvils, as in real systems. Prognostic condensates and separation between microphysics and transport become a vehicule for an easier representation of the memory of the convective cells and of the convectively-generated cirrus.

Triggering, entrainment-detrainment rates, normalized convective fraction along the vertical, and mass flux closure are designed as explicit functions of convective vertical velocity, itself being driven by buoyancy. This allows a continuous formulation of convection from dry thermals to deep precipitating events.

This convection scheme is part of the physics designed for the CMIP6 simulation exercise and for operational ensemble forecasting at Meteo-France (NWP and seasonal) with the ARPEGE GCM. The present article (Part I) presents equations and demontrates cloud budgets. The second article (Part II) presents results in 1D and 3D experiments.

Key Words: convection, parameterization, microphysics

1. Introduction

Convection is a major atmospheric process, that involves water vapour fluxes, condensation, latent heat release, and impacts wind fields. Clouds are associated with convection and turbulence on scales of meters to kilometers, smaller than current GCMs (Global Climate Models) resolution. Convective parameterizations have been developed to quantify the effect of these sub-grid-scale processes on the resolved model scale. Several challenges raised for convective parameterizations:

- diurnal cycle of convection: most parameterizations predict this cycle with a phase lead with respect to observations, as shown by Guichard et al. (2004), Peatman et al. (2015) and others.
- sensitivity of deep convection to mid-tropospheric moisture: Derbyshire et al. (2004) found that, for identical temperature profiles, CRMs made a transition from shallow to deep convection as free tropospheric relative humidity increased, a point still difficult to predict by most convective parameterizations.
- precipitation regime: getting precipitation PDF right, and day-to-day, weekly, monthly variations, is challenging, as most GCMs underestimate variability, see for example Lin et al. (2006) for an IPCC GCMs comparison.
- as resolutions are continuously improving along the years, the convective parameterization exercise enters the so called "grey-zone", where convection can no longer be considered as stationnary with respect to the resolved forcing, the parameterization should therefore handle a convective memory, keep and transfer this memory from one time-step to the next, from one grid-point to its neighbours, which promotes the use of prognostic variables.

Getting these 4 points right turns out to be a complex problem. Our guidelines, for the present proposal, are

- increasing the number of prognostic condensates variables, to deal inside convective updraft with the same level of sophistication as in the resolved scale microphysics (autoconversion, aggregation, collection, riming, melting, etc), as in Lopez (2002) and Bouteloup et al. (2011).
- separating microphysics and transport in grid-scale equations, as proposed by Piriou et al. (2007), to release stationnary cloud budget assumptions, and make it possible to call a separate microphysics scheme,
- make updraft vertical velocity drive both entrainment-detrainment values and closure, as in Guérémy (2011) to avoid as much as possible ad-hoc tuned entrainment or closure formulas that may become questionable in a climate change prediction exercise.

The new prognostic microphysical variables and the separation microphysics - transport make it possible to handle strong internal positive feedbacks, despite a small number of tuning parameters. In the next sections we present the equations, discuss the feedbacks introduced, and demonstrate cloud budgets. Results in 1D and 3D simulations are presented in Part II.

2. Microphysics and transport equations

CSRM (Cloud Systems Resolving Models) equations for water vapor (q), static energy ($s = c_p T + g\,z$) and horizontal wind (u, v) may be expressed in generic form as

$$\begin{aligned}
\frac{\partial q}{\partial t} &= ED_q - C + E_C + E_P - \left(\vec{u}\cdot\vec{\nabla}\right) q \\
\frac{\partial s}{\partial t} &= ED_s + R + L\,(C - E_C - E_P) + H - \left(\vec{u}\cdot\vec{\nabla}\right) s \\
\frac{\partial u}{\partial t} &= \dot{u}_p - \left(\vec{u}\cdot\vec{\nabla}\right) u \\
\frac{\partial v}{\partial t} &= \dot{v}_p - \left(\vec{u}\cdot\vec{\nabla}\right) v
\end{aligned} \tag{1}$$

where ED is turbulent source/sink (Eddy Diffusivity), C is condensation (≥ 0), E_C evaporation of cloudy condensates (≥ 0), E_P precipitation evaporation (≥ 0), R is the radiative source/sink, H is the heat source/sink due to precipitation (sensible heat exchanges between falling drops and surrounding air, latent heat release due to melting/freezing), $\dot{u}_p$ and $\dot{v}_p$ are the momentum net sources due to pressure force, rotation, turbulence.

Following Piriou et al. (2007) we can derive a simpler system from the one above, relevant for subgrid-scale convective parameterization, expressing grid-scale tendencies due to sub-grid scale convective processes; this system, called MTCS (Microphysics and Transport Convective Scheme), is obtained while neglecting, here and for the sake of simplicity, momentum sources, and expressing the mean effect of advection as a double flux divergence term (updrafts and environment; in this article downdrafts will be omitted from equations for convenience, to shorten the equations, as they have a symmetric form like that of updrafts; equations are also presented under the assumption of a small updraft area fraction ($\alpha \ll 1$), thus replacing environmental values by grid-scale ones):

$$\begin{aligned}
\left(\frac{\partial \overline{q}}{\partial t}\right)_{conv} &= -C + E_C + E_P - \frac{\partial}{\partial p}\alpha\,\omega_c(q_c - \overline{q}) \\
\left(\frac{\partial \overline{s}}{\partial t}\right)_{conv} &= L\,(C - E_C - E_P) + H - \frac{\partial}{\partial p}\alpha\,\omega_c(s_c - \overline{s}) \\
\left(\frac{\partial \overline{u}}{\partial t}\right)_{conv} &= - \frac{\partial}{\partial p}\alpha\,\omega_c(u_c - \overline{u}) \\
\left(\frac{\partial \overline{v}}{\partial t}\right)_{conv} &= - \frac{\partial}{\partial p}\alpha\,\omega_c(v_c - \overline{v})
\end{aligned} \tag{2}$$

where α is the updraft surface fraction and ω_c the updraft vertical velocity. ψ_c and $\overline{\psi}$ are respectively the updraft value and the grid-scale value of the variable ψ. The parameterization exercise consists in formulating α, ω_c, ψ_c (section 3) and microphysics related terms (sections 4 and 5). This equation set is relevant for dry convection, nonprecipitating convection (cumulus) and precipitating convection (cumulus, cumulonimbus). The production of precipitation is performed through a microphysics scheme (see sections 4 and 5) as in CSRMs.

Such a system, when used in the convective parametrization, makes it possible to validate the parameterization prediction beyond quantities like Q1, Q2 or Q3, as CSRMs provide without any additional hypothesis (i) transport terms like $\overline{w'q'}$, $\overline{w'\theta'}$ or $\overline{w'u'}$ and (ii) microphysical terms (condensation, autoconversion, collection, precipitation evaporation, etc), which can be compared to those provided by system (2). Transport and microphysics can be validated separately. An example of such a validation is presented in section 8.

3. Convective profile, prognostic vertical velocity and closure condition

Most of the content of this section is taken from Guérémy (2011). For the sake of self-sufficiency of the present paper, the salient points are summarized in the following, including some improvements made since.

The convective vertical velocity is computed following Simpson and Wiggert (1969) and De Hui and Bougeault (1992) as

$$\frac{\partial \omega_c}{\partial t} = -\frac{1}{2}\frac{\partial {\omega_c}^2}{\partial p} - \frac{\rho\, g^2}{(1+\gamma)}\frac{T_{vc} - \overline{T}_v}{\overline{T}_v} + (\epsilon_t + \epsilon_o + K_d)\,{\omega_c}^2 \tag{3}$$

where $T_{vc} = T_c(1 + 0.608\,q_{vc} - q_{lc})$ is the updraft virtual temperature, $\overline{T}_v = \overline{T}(1 + 0.608\,\overline{q_v} - \overline{q_l})$ the grid averaged virtual temperature, γ a virtual mass parameter ($\gamma = 0.5$, following Simpson (1971)) and K_d an aerodynamic drag parameter.

Entrainment E and detrainment D are decomposed into two parts corresponding to the two different scales at which these processes occur.

$$E = E_o + E_t, \quad D = D_o + D_t \tag{4}$$

Following Tiedtke (1989), the first part, called the organized entrainment and detrainment (subscript o), consists of the mixing due to the flow associated with mesoscale convergence and divergence. The second part, called the turbulent entrainment and detrainment (subscript t), represents the mixing due to turbulent exchanges around the edges of the convective part of the grid; turbulent entrainment and detrainment rates are assumed to be equal. Fractional entrainment and detrainment rates (both organized and turbulent) are defined following Turner (1963) as

$$E = M\epsilon, \quad D = M\delta. \tag{5}$$

where $M = -\alpha\,\omega_c$ is the mass flux.

The bulk ascent profile is defined, starting from the bottom of the atmosphere, along an ascending process that can be dry (below cloud base) or moist pseudo-adiabatic (over cloud base), taking into account the effect of entrainment on updraft properties:

$$\frac{\partial \psi_c}{\partial \phi} = \rho\,(\epsilon_t + \epsilon_o)\,(\overline{\psi} - \psi_c) \tag{6}$$

where ψ is the temperature, the specific humidity or the components of horizontal velocity. In the last case, the pressure gradient effect might taken into account following Kershaw and Gregory (1997). The choice between dry and moist ascent mode will be made by comparing the temperatures at the top of the layer (if the moist pseudo-adiabat temperature is higher than that of the dry adiabat, the lifting condensation level (LCL) is located in the present layer), thus allowing an internal adaptive treatment of dry and moist ascent. The equations are the

following:

$$C_p dT_c + d\phi_c = 0, \;\; C_p dT_c + d\phi_c + L dq_{vc} = 0, \tag{7}$$

conservation of dry and moist static energy. The cloud vertical velocity being obtained on the top variable level of the layer considered, the turbulent fractional entrainment rate is defined on that level as

$$\epsilon_t = \epsilon_{tn} + (\epsilon_{tx} - \epsilon_{tn}) f_\epsilon(\omega_c, \omega_{cx}, \omega_{cn}), \tag{8}$$

where ϵ_{tn} is a minimum value ($\epsilon_{tn} = 0.5 \times 10^{-4}\, m^{-1}$), ϵ_{tx} is a maximum value ($\epsilon_{tx} = 9 \times 10^{-4}\, m^{-1}$), $f_\epsilon(\omega_c, \omega_{cx}, \omega_{cn})$ is an analytical monotonic function of ω_c which is equal to 1 when $\omega_c \geq \omega_{cx}$ ($\omega_{cx} = -2\, Pa\, s^{-1}$), and to 0 when $\omega_c \leq \omega_{cn}$ ($\omega_{cn} = -27.5\, Pa\, s^{-1}$); f_ϵ is a sine squared. Equation 8 allows both shallow and deep convection to be handled, providing a large (small respectively) value of entrainment for shallow (deep respectively) convective ascent characterized by small (large respectively) absolute value of p vertical velocity, as proposed by Tiedtke (1989) for example, but using a continuous transition in the present scheme.

The K_d aerodynamic drag parameter has the same dependency to vertical velocity: it is computed as

$$K_d = \frac{\epsilon_t}{\epsilon_{tn}} K_{dn} \tag{9}$$

where $K_{dn} = 2.9 \times 10^{-4}\, m^{-1}$.

Organized entrainment and detrainment rates are obtained from the stationarized mass conservation relation, modulated by a buoyancy-sorting process following the work of Bretherton et al. (2004): the mass conservation is expressed as

$$\frac{\partial M}{\partial p} = D - E, \tag{10}$$

which directly provides a maximum value for the organized entrainment-detrainment rate

$$(\epsilon\delta)_{ox} = |\frac{1}{\omega_c} \frac{\partial \omega_c}{\partial p}|. \tag{11}$$

A factor μ_0 (between 0 and 1) partitioning positively versus negatively buoyant mixtures is computed according to the buoyancy-sorting approach, in order to get the final expression of both organized entrainment and detrainment rates as

$$\epsilon_0 = (\epsilon\delta)_{ox}\, \mu_0^2, \;\; \delta_0 = (\epsilon\delta)_{ox}\, (1 - \mu_0)^2. \tag{12}$$

The buoyancy-sorting process is not considered as long as the maximum organized entrainment rate is sufficiently larger than its turbulent counterpart to allow the ascent of some negatively buoyant parcels, *i.e.*

$$(\epsilon\delta)_{ox} > K_\epsilon\, \epsilon_t, \tag{13}$$

with $K_\epsilon = 1.75$. Such a definition of organized entrainment and detrainment rates enables a computation of a normalized convective fraction along the vertical σ, starting from 1 at the convective base and decreasing with height (instead of being constant equal to 1, in absence of buoyancy-sorting), using the mass conservation relation as

$$\frac{1}{\sigma\, \omega_c} \frac{\partial \sigma\, \omega_c}{\partial p} = \delta_0 - \epsilon_0, \tag{14}$$

with $M = -a\, \sigma\, \omega_c$, a being a constant (the convective fraction at base of convection is $\alpha = a\, \sigma$).

Organized entrainment and detrainment rates were designed partly following the work of Bretherton et al. (2004). They are based on a buoyancy-sorting approach assuming that the lateral mixing of the updraft and its environment generates a spectrum of mixtures. Buoyancy-sorting is used to determine which mixtures are incorporated into the updraft and which are rejected, as in Guérémy (2011) equations (26) to (31).

Closure is referred in the litterature as defining the convective intensity in a given parameterization, quantified by bulk mass flux $M = -\alpha\, \omega_c$. As reviewed by Yano et al. (2013), closure is still considered an overall unresolved problem. In the PCMT development process, several closures have been introduced and tested: humidity convergence based, saturation deficit (over the PBL) based, CAPE-based, etc. The CAPE-based closure from Guérémy (2011) appeared to have the highest generality in our tests, in the sense of producing reasonable results when running with same tunings both 1D cases (see Part II of this article) and 3D GCM climate simulations. This closure is based on a CAPE relaxation time τ, whose value is computed as the ratio between convective vertical extension and mean convective vertical velocity, modulated by a function of the resolution in order to keep the same magnitude between the mass flux and the resolved vertical velocity, which is itself proportional to the resolution (through the continuity equation).

Downdrafts are diagnostic, following Guérémy (2011). Convective cloudiness is parameterized as proportional to convective area fraction: $n = \beta\, \alpha$, with $\beta = 10$.

4. Prognostic condensates equations

The convective prognostic variables are liquid water q_{lc}, ice water q_{ic}, rain q_{rc} and snow q_{sc}; the same prognostic variables are defined in the convective environment: liquid water q_{le}, ice water q_{ie}, rain q_{re} and snow q_{se}, see Figure 1. These 8 prognostic variables are defined and advected in 3D by the host model.

Liquid water, convective and environment:

$$\begin{aligned}
\frac{\partial}{\partial t}\overline{q_{lc}} &= \text{Advec}(\overline{q_{lc}}) - \frac{\partial \omega_c\, \overline{q_{lc}}}{\partial p} \\
&\quad + E\, q_{le} - D\, q_{lc} + \text{C}_{lc} - \text{AC}_{lc} + \text{MI}_{lc} \\
\frac{\partial}{\partial t}\overline{q_{le}} &= \text{Advec}(\overline{q_{le}}) - \frac{\partial \omega_{ce}\, \overline{q_{le}}}{\partial p} \\
&\quad - E\, q_{le} + D\, q_{lc} + \text{C}_{le} - \text{AC}_{le} + \text{MI}_{le} \\
C_{lc} &= -\alpha\, \omega_c\, (1 - f_i)\, \frac{\partial q_{vc}}{\partial p} \\
\overline{q_{lc}} &= \alpha\, q_{lc} \\
\overline{q_{le}} &= (1 - \alpha)\, q_{le}
\end{aligned} \tag{15}$$

where Advec is the 3D host model advection, E entrainment, D detrainment, C_{lc} condensation, AC Autoconversion-Collection, MI Melting-Icing. The convective condensation rate C_{lc} is parameterized using the diagnostic profile of convective water vapour gradient $\frac{\partial q_{vc}}{\partial p}$ coming out from the vertical integration of the pseudo-adiabatic ascent (7). f_i is the fraction of ice (versus liquid), between 0 and 1, to allow the coexistence of liquid and solid cloud condensate, as in equation (3) from Lopez (2002) . The environmental condensation rate C_{le} is computed following Smith (1990). The convective vertical velocity in the environment ω_{ce} is computed while closing the mass budget in each model grid cell:

$$\alpha\, \omega_c + (1 - \alpha)\, \omega_{ce} = 0 \tag{16}$$

Ice water, convective and environment:

$$\begin{aligned}
\frac{\partial}{\partial t}\overline{q_{ic}} &= \text{Advec}(\overline{q_{ic}}) - \frac{\partial \omega_c \overline{q_{ic}}}{\partial p} \\
&\quad + E\, q_{ie} - D\, q_{ic} + \text{C}_{ic} - \text{AC}_{ic} + \text{MI}_{ic} \\
\frac{\partial}{\partial t}\overline{q_{ie}} &= \text{Advec}(\overline{q_{ie}}) - \frac{\partial \omega_{ce} \overline{q_{ie}}}{\partial p} \\
&\quad - E\, q_{ie} + D\, q_{ic} + \text{C}_{ie} - \text{AC}_{ie} + \text{MI}_{ie} \\
C_{ic} &= -\alpha\, \omega_c\, f_i\, \frac{\partial q_{vc}}{\partial p} \\
\overline{q_{ic}} &= \alpha\, q_{ic} \\
\overline{q_{ie}} &= (1-\alpha)\, q_{ie}
\end{aligned} \tag{17}$$

Rain, convective and environment:

$$\begin{aligned}
\frac{\partial}{\partial t}\overline{q_{rc}} &= \text{Advec}(\overline{q_{rc}}) + S_{rc} \\
&\quad + E\, q_{re} - D\, q_{rc} + \text{AC}_{lc} - \text{Ev}_{rc} + \text{MI}_{rc} \\
\frac{\partial}{\partial t}\overline{q_{re}} &= \text{Advec}(\overline{q_{re}}) + S_{re} \\
&\quad - E\, q_{re} + D\, q_{rc} + \text{AC}_{le} - \text{Ev}_{re} + \text{MI}_{re} \\
\overline{q_{rc}} &= \alpha\, q_{rc} \\
\overline{q_{re}} &= (1-\alpha)\, q_{re}
\end{aligned} \tag{18}$$

Snow, convective and environment:

$$\begin{aligned}
\frac{\partial}{\partial t}\overline{q_{sc}} &= \text{Advec}(\overline{q_{sc}}) + S_{sc} \\
&\quad + E\, q_{se} - D\, q_{sc} + \text{AC}_{ic} - \text{Ev}_{sc} + \text{MI}_{sc} \\
\frac{\partial}{\partial t}\overline{q_{se}} &= \text{Advec}(\overline{q_{se}}) + S_{se} \\
&\quad - E\, q_{se} + D\, q_{sc} + \text{AC}_{ie} - \text{Ev}_{se} + \text{MI}_{se} \\
\overline{q_{sc}} &= \alpha\, q_{sc} \\
\overline{q_{se}} &= (1-\alpha)\, q_{se}
\end{aligned} \tag{19}$$

where S_r and S_s are the sedimentation of rain and snow, following Bouteloup et al. (2011).

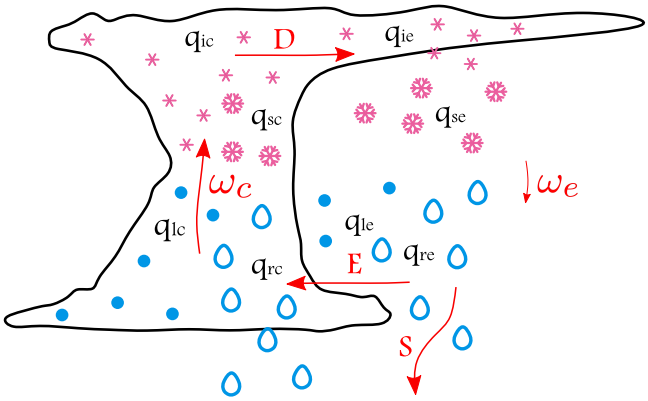

Figure 1. The 8 prognostic condensates from equations 15 to 19. Entrainment E is an horizontal process that imports all environmental variables (liquid, ice, snow, rain) into the convective updraft. Detrainment D is the symmetrical process that detrains horizontally convective variables into the environment. Sedimentation S is a vertical process which applies to convective and environmental snow and rain.

The microphysics scheme, that computes terms Ev, AC and MI from equations 15 to 19, is called twice: once on the convective profile (subscript c), once on the environmental profile (subscript e). When no convection is active, like in stable dry profiles or stable moist air ascents, there is no source of q_{lc} or q_{ic}, as $\omega_c = 0$ and therefore $C_{lc} = C_{ic} = 0$. In this case the only significant condensates are the environmental ones (q_{le}, q_{ie}, q_{re}, q_{se}) which deal with stratiform condensation due to resolved ascents or radiative cooling (fog).

Introducing these 8 prognostic condensates (4 convective ones, 4 environmental ones) activates many feedbacks, among these:

- Convective condensates are detrained into the environment, making convective precipitation strongly sensitive to mid-tropospheric moisture: when environment is wet, a large part of cloud condensates detrained near cloud top (where D is large due to buoyancy-sorting) saturates the environment, and soon generates stratiform snow and rain, as in real convective systems. When environment is dry, convective condensates are smaller due to updraft entrainment E, in addition a large part of detrained condensates (liquid, ice, rain, snow) will be evaporated in the environment by the microphysics scheme.
- This sensitivity also applies for the transitory state, when convection develops: surface precipitation will start only when large enough condensation rate can generate cloud contents over the autoconversion thresholds, and when these rain and snow generated can sedimentate through non-saturated levels, below cloud base (for q_{rc} or q_{sc}) or in the environment (for q_{re} or q_{se}), where they may be fully evaporated (virga). This delays the diurnal phase of surface precipitation.
- The transition between moist non-precipitating shallow convection and precipitating convection is delegated to the microphysics scheme, which decides whether autoconversion is active.

Delegating microphysics to a separate microphysics scheme activates new feedbacks and makes the mere convection scheme simpler, as it focuses on computing mass flux $-\alpha\,\omega_c$ and condensation rates (C_{lc} and C_{ic}). The microphysics may be sophisticated, close and consistent to CSRMs or LES ones. This also permits a faster adaptation of convection schemes to research improvements in microphysics.

5. Microphysics

The microphysics is called twice: with convective profile (q_{vc}, q_{lc}, q_{ic}, q_{rc}, q_{sc}, T_c) and with environmental profile (q_{ve}, q_{le}, q_{ie}, q_{re}, q_{se}, T_e). This microphysical scheme was first developed by Lopez (2002). It is based on the approach of Fowler and Randall (1996) where any time-stepping is overcome by the use of a Lagrangian scheme for the fall of rain and snow. The microphysical scheme uses a prognostic treatment of precipitation to provide a finer description of the temporal evolution of the vertical distribution of precipitation and, thus, of the effects of latent-heat release associated with sublimation and evaporation. In the current version the sedimentation Lagrangian scheme was replaced by a technical based on the works of Rotstayn (1997), Geleyn et al. (2008) and Bouteloup et al. (2011). In that kind of sedimentation scheme the precipitation flux is computed diagnostically from the top to the bottom of the atmosphere. The sedimentation equation is replaced by three probabilities of transfer associated with the following types of precipitation: (i) precipitation present in the layer at the beginning of the time step ; (ii) precipitation coming from the layer above and crossing the layer under consideration and (iii) precipitation produced locally during the time step. These schemes are unconditionally stable. The probabilities of transfer needed by the scheme can be built from the sedimentation equation as in Rotstayn (1997), based on a PDF of fall speeds as in Geleyn et al. (2008) or defined to mimic Eulerian or Lagrangian sedimentation algorithms as in Bouteloup et al. (2011).

6. Algorithmics and intra time-stepping

The vertical transport of liquid water q_{lc} and ice water q_{ic} (terms $-\frac{\partial \omega_c\, q_{lc}}{\partial p}$ and $-\frac{\partial \omega_c\, q_{ic}}{\partial p}$ from equations 15 and 17) is challenging, as convective vertical velocity multiplied by GCM or LAM time-steps lead to CFLs (Courant-Friedrich-Levy) larger than 1. The

statistical sedimentation algorithm from Bouteloup et al. (2011) originally designed for rain and snow sedimentation, is used also for vertical transport of q_{lc} and q_{ic}, replacing sedimentation speed by convective velocity, and rain or snow contents by liquid and ice ones.

Intra time-stepping: q_l, q_i, q_r and q_s -convective and environment- from previous time-step are first updated from entrainment-detrainement processes (E and D in the equations above), then from condensation (C_{lc} and C_{ic}). They enter microphysics (autoconversion, collection, etc) and are updated by these processes. Vertical transport is applied to these updated values. As liquid water may be transported above freezing level, or the reverse (ice water being transported below freezing level in the environment), variables are finally updated from icing-melting adjustment.

Adding the 5 convective prognostic variables (4 convective condensates plus convective vertical velocity, the environmental ones are already activated in the ARPEGE GCM control model) leads to an increase of 10% computation time and 7% memory use of the whole model. The computation time change is mainly due to the 3D semi-lagrangian advection of the new prognostic variables.

7. SCM tuning of some key parameters

The scheme validation is carried out in a SCM mode framework using ARPEGE-Climat on selected case studies, representative of different convective regimes. It is considered to be the first necessary step in order to provide numerical values of the scheme parameters; indeed, SCM simulations allow a detailed analysis of the physical processes against both observations and explicit simulations (Bechtold et al. (2000), Derbyshire et al. (2004), Guichard et al. (2004), Duynkerke et al. (2004)). In a second step, a first order evaluation is performed using SCM simulations of additional case studies. The main goal of this evaluation is to ensure the relevance of the parameter choice undertaken in the previous step. In between those two steps, an intermediate one has been devised to define 2 parameters among those providing the most sensitive response of the scheme: the turbulent entrainment rate (its maximum value ϵ_{tx} from equation 8) and the precipitation efficiency (the solid auto-conversion rate). Two sensitivity experiments result from this choice. The analysis of these two experiments will be discussed throughout the evaluation process, from and beyond the SCM mode framework.

7.1. *Definition of the scheme parameters*

The main parameters of PCMT (those providing the most sensitive response) are the aerodynamic drag parameter (its minimum value K_{dn} from equation 9), the turbulent entrainment rate (its maximum value ϵ_{tx} from equation 8) and the solid auto-conversion rate (AC_s), as defined in equation 5 from Lopez (2002). Further to these three parameters, a tunable factor of the resolution function included in the CAPE closure expression (see Guérémy (2011) page 691), has also been tuned. This has been done considering SCM case studies (knowing the resolution of their prescribed forcings), together with GCM simulations performed at different spatial resolutions. Nevertheless, it will not be discussed in details here.

7.2. *Aerodynamic drag parameter K_d : TOGA case*

The TOGA SCM case study (Bechtold et al., 2000) has been chosen, because it is representative of a typical tropical deep convection development. Furthermore, this SCM case study is well constrained by the total dynamical tendencies obtained from a CRM simulation. The parametrised mass flux will be therefore perfectly controlled by the forcing. And it turns out that K_d is a key parameter in the computation of the convective vertical velocity (see equation 3). The minimum value of K_d (K_{dn}) is considered here; K_d is computed using the same expression as the turbulent entrainment rate ϵ_t between K_{dn} and K_{dx}, the range between the maximum and minimum being the same as that of ϵ_t (equation 9). The smaller the drag (*i.e.* the parameter K_{dn}), the deeper the convection. Figure 2 shows the SCM averaged mass flux profile (sum of updraught and downdraught) over the last hour of simulation (i.e. hour 7), compared to the CRM's one from Bechtold et al. (2000). The nominal value of K_{dn} is equal to $4. \times 10^{-5}\, Pa^{-1}$. The mass flux profiles obtained with this nominal value $\pm 50\%$ are also depicted in Figure 2. There are two CRM mass profiles in Figure 2, the first one corresponding to the total and the second to its updraught convective contribution, according to the sampling criterion used to define this contribution out of the CRM simulation. The nominal SCM mass flux profile presents a convective part together with a stratiform part aloft, being in between the two CRM profiles. The SCM downdraught mass flux is weak compared to its updraught counterpart (not shown). The expected response to a decrease-increase of K_{dn} is clearly seen in Figure 2: deeper and weaker the convection with a K_{dn} decrease and vice-versa. The lower intensity is due to the fact the convection is consuming the same amount of CAPE provided by the imposed forcing, but over a deeper depth.

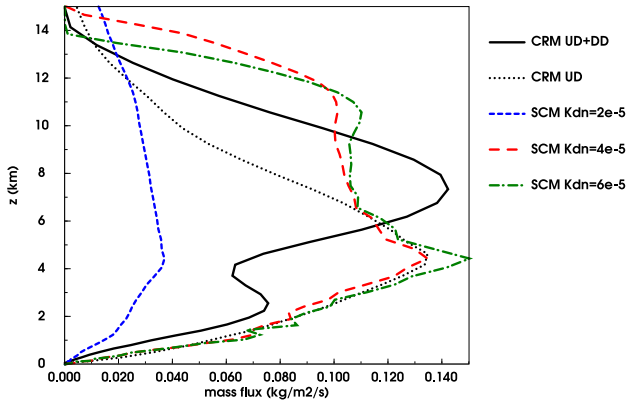

Figure 2. TOGA SCM Case. SCM and CRM mass flux profiles, averaged over hour 7. Nominal K_{dn} and $\pm 50\%$ for SCM; total and updraught convective contribution for CRM.

The temperature and specific humidity tendencies at the end of the SCM 7-hour simulation represent a relevant metric to assess the convective skill (Figure 3), as the CRM simulation was in quasi-equilibrium. These vertical profiles appear to be among the best profiles resulting from the SCM inter-comparison reported in Bechtold et al. (2000) (see their Figure 6).

7.3. *Turbulent entrainment rate ϵ_{tx} : BOMEX case*

To define the optimal value of the maximum turbulent entrainment rate ϵ_{tx} from equation 8, the BOMEX SCM case study (Siebesma and Cuijpers (1995), hereafter called SC95) has been chosen. This is a typical case of trade wind shallow convection. The two main forcings are a large-scale subsidence together with a radiative cooling of $-2\,K\,day^{-1}$. There is also a low level horizontal drying below $500\,m$ (see Figure 2 of SC95). The surface flux scheme after Louis (1979) is interactive, the sea surface temperature being prescribed as $300.4\,K$. In SC95, the two authors performed a large-eddy simulation (LES), followed by a diagnostic of convective scheme characteristics such as mass flux and entrainment-detrainment rates, using specified decompositions between convective and environment parts in their simulation. Figure 4 shows the total SCM detrainment rate profile

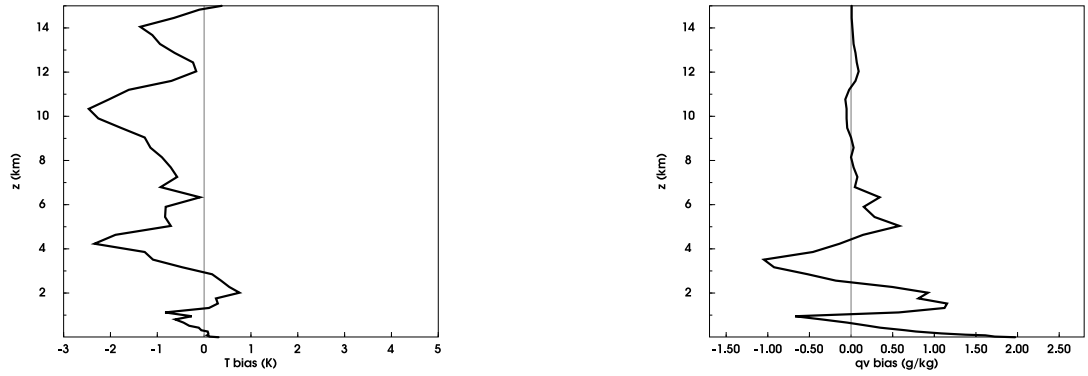

(a) Temperature tendency

(b) Specific humidity tendency

Figure 3. TOGA SCM Case. Tendency between initial and final profiles (at the end of the 7-hour simulation) for temperature and specific humidity.

(averaged between 8 and 24 h, i.e. the stationary phase of the SCM simulation, the physics balancing the prescribed dynamical forcings for this case study), compared to the one diagnosed from the LES. The SCM profiles obtained with the ϵ_{tx} optimal value of $9. \times 10^{-5} Pa^{-1}$ and two surrounding others within $\pm 50\%$ are plotted in Figure 4. The optimal value of the minimum turbulent entrainment rate has been set to $\epsilon_{tn} = 0.5 \times 10^{-5} Pa^{-1}$ following Bougeault (1985), giving rise to a range of 18 between the extrema (as for the aerodynamic drag parameter, see previous sub-section). The expected response to a decrease-increase of ϵ_{tx} is clearly seen in Figure 4: deeper the convection with a ϵ_{tx} decrease and vice-versa. The top convection lies around 2 km according to SC95. This is the case for the SCM simulation using the optimal value of ϵ_{tx}, with reasonable detrainment rates between 500 and 1000 m, whereas the convection top is located too low, with larger entrainment rates between 500 and 1000 m using the excess ϵ_{tx} value (and vice-versa).

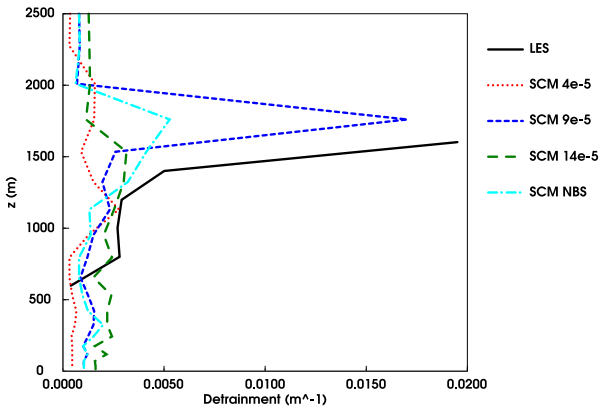

Figure 4. BOMEX SCM case. SCM and LES detrainment rates profiles, averaged between 8 and 24h. Nominal ϵ_{tx} ($9. \times 10^{-5} Pa^{-1}$) and $\pm 50\%$ for SCM. SCM NBS stands for the nominal ϵ_{tx}, with No Buoyancy-Sorting.

Figure 4 also shows the benefit, for shallow cumulus clouds, of activating the buoyancy-sorting process in the entrainment-detrainment computation, by comparing mixed (SCM NBS) to short-dashed (SCM $9. \times 10^{-5} Pa^{-1}$) curves. Buoyancy-sorting acts as a modulation of the organized entrainment-detrainment computation (equation 12), which allows the convective plume to detrain lower in the updraught (inducing a light moistening of the environment, suitable for an increased convective development), instead of going directly from an all entraining to an all detraining plume. As a consequence, the detrainment near cloud top has a larger magnitude.

Figures 5 and 6 show the importance, as validating any convective parameterization on this BOMEX case, of the surface latent heat flux. This flux has to be predicted from a surface scheme. We run two experiments: the PCMT reference simulation and a perturbed one. In the perturbed simulation the parameter of subgrid-scale effects in the surface flux scheme has been set to zero; this parameter is a factor of the ratio between the actual momentum exchange coefficient and its neutral value (being a measure of surface instability), giving rise to an additional contribution to the roughness length in the computation of the final exchange coefficient from the Louis (1979) scheme. The perturbed simulation has lower surface heat flux (Figure 5), farther from the $150\, W\, m^{-2}$ suggested by LES runs (Siebesma and Cuijpers (1995), Siebesma et al. (2003)). For the reference simulation (Figure 6 (a)), a stationary shallow cumulus is obtained after a 8 h spin-up, with a cloud base just below 500 m and a cloud top reaching 2000 m, in agreement with observation and several LES (Siebesma et al. (2003)). The cloud fraction decreases with height from about 15% to 1%, in accordance with what has been observed and explicitly simulated. In the perturbed simulation (Figure 6 (b)) the cumulus cloud has a too large cloudiness at cloud base; this is the consequence of a latent heat flux being decreased by 20% compared to the reference simulation (100 versus $125\, W\, m^{-2}$). On this BOMEX case, the larger the surface heat flux, the stronger the convection, resulting in more vertical transport and less low shallow cloudiness.

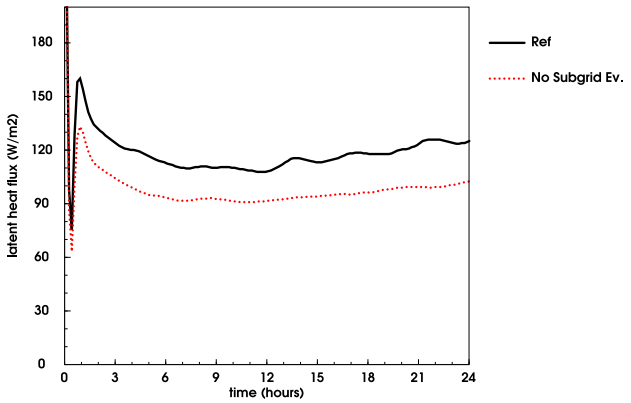

Figure 5. BOMEX SCM case. Latent heat fluxes, for a reference prediction and for a perturbed one, in which surface latent heat is reduced (no subgrid-scale term in the surface fluxes).

Figure 7 shows profiles of convective quantities (averaged between 8 and 24 h) directly impacting the resolved variables: convective mass flux entering both in the condensation and transport terms (Figure 7 (a)), together with physical (turbulence and convection) temperature and specific humidity tendencies (Figure 7 (b) and (c)). In Figure 7 (a), the SCM convective mass flux is compared to that obtained from the LES as for the entrainment (see Figure 4), whereas in Figure 7 (b) and (c), the

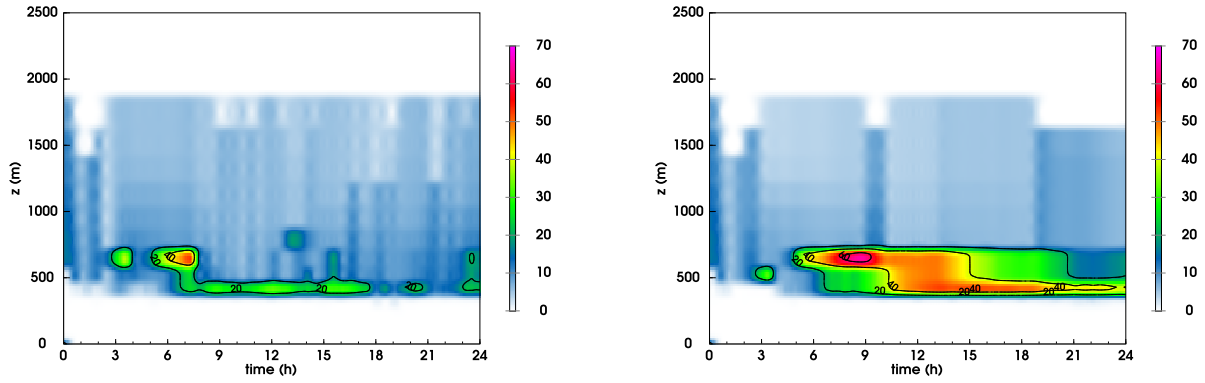

(a) Reference simulation cloud fraction.

(b) Perturbed simulation without subgrid-scale term in the surface fluxes.

Figure 6. BOMEX SCM case. Time evolution of SCM cloud fraction (%), for a reference prediction and for a perturbed one, in which surface latent heat is reduced.

convective tendencies are compared to the ones diagnosed from the observations (see Figure 4 of SC95). The convective mass flux appears to be three times less intense than the LES one, but displaying the same vertical shape, the maximum being located around 650 m. The weaker SCM convection is related to weaker simulated surface fluxes compared to observed and LES ones. Increasing the SCM surface fluxes with the help of a subgrid-scale parameter tuning (see previous paragraph) tends to slightly improve the simulated results (not shown). The tendencies from the physics (Q1 and Q2 terms) compare reasonably well with observed ones. For the Q1 profile, the radiative contribution is not included because it is considered to be a prescribed forcing term reaching $-2\,K\,day^{-1}$. These tendencies are less intense than observed above 1500 m, which is also the case for the LES one (see Figure 4 of SC95); SCM simulation and LES are indeed closer due their identical initialization profile, being set in the northern part of the field campaign domain known to be less energetic in terms of surface fluxes.

Specific humidity profiles at the beginning and at the end of the SCM simulation (24 h) are depicted in Figure 8. The results of the control simulation together with those taking ϵ_{tx} $\pm 50\%$ into account are plotted. As the considered case study is stationary, it provides a measure of the bias at the end of the simulation. The control simulation tends to be too dry between 1000 and 1500 m and too moist below 500 m, due to an excess drying aloft and moistening below during the first 8 hours of simulation (not shown). As a consequence of the changes induced in the entrainment rates by a decrease-increase of ϵ_{tx} (see above), the specific humidity profile is too moist (dry respectively) in the upper part of the convective layer (above 1700 m), while being dryer (moister respectively) than the control around 1000 m.

7.4. Autoconversion rate AC_s : EUROCS idealized humidity case

In order to determine the optimal value of the solid auto-conversion rate AC_s (as defined in equation 5 from Lopez (2002)), a convective four case study in one has been selected: Derbyshire et al. (2004), hereafter called D04. This is an idealized SCM case study designed to investigate the sensitivity of moist convection to environmental humidity. The convection scheme described in Guérémy (2011), being partly at the origin of PCMT, was one of the schemes used in D04. The prescribed forcings consist of a nudging of the prognostic variables toward a specified profile corresponding to a moderate instability to adiabatic moist ascent for the temperature, using four different constant values of relative humidity (RH) in the free troposphere (25, 50, 70 and 90%). As for the BOMEX case study, the SCM simulations are reaching a stationary state after a spin-up phase, the surface fluxes being computed over an ocean surface defined by a given SST. Two CRM have provided simulations of this case study, and their results are considered as references to assess the performance of the SCM runs (D04).

Figure 9 compares the mean surface precipitation over the quasi-steady period from the CRM (mean of the two models) and SCM (time averaged between 12 and 24 h). The 3 RH largest values have been reported in the table, as so far as the 25% case is not producing significant precipitations. An AC_s nominal value of $35 \times 10^{-4}\,s^{-1}$ (corresponding to a characteristic time of about 5 mn) has been chosen, providing the best SCM results using the CRM as reference, compared to the SCM results obtained with this nominal value $\pm 57\%$. The increase of the precipitation obtained with an increase of AC_s was expected, showing that this parameter is relevant in terms of testing the scheme sensitivity to the precipitation efficiency (see Part II).

Further to the assessment of surface precipitation, it is worth to validate the behaviour of the scheme in terms of heating and moistening. Figure 10 shows, for the 4 values of the environmental RH, the apparent heat source (Q1) and the apparent moisture sink (Q2). This figure must be compared to the ones produced using the CRM (Figures 5 and 6 from D04). The PCMT convection scheme is able to simulate the proper sensitivity to the environmental humidity, going progressively from shallow to deep convection as RH increases in the environment. Figure 11 shows that a significant part of precipitation is obtained from the environment part; the source of this environmental rain $\overline{q_{re}}$ from equation 18 and 19 being the detrainment of all convective species (water vapour, liquid, ice, rain, snow), through their direct effect ($D\,q_{rc}$ and $D\,q_{sc}$) or indirect effects (feeding the AC_{le} and AC_{ie} terms). Detrainment of convective prognostic variables, and evaporation of the resulting environmental prognostic variables strongly depends on environmental relative humidity, contributing to this proper response of the scheme in predicting convection sensitivity to humidity.

8. Demonstrating cloud budgets

Figures 12 to 20 show the budget of the 8 prognostic condensates and of temperature over an ARPEGE GCM 3 days prediction, horizontally averaged over the Tropics ($30^\circ S$ to $30^\circ N$). Entrainment-detrainment processes are by construction of equations 15 to 19 conservative, having the opposite sign for convective and environmental variables. The same stands for icing-melting, which converts liquid into ice and reversely. Positive values of convective vertical transport of q_{lc} span much higher than iso $0^\circ C$, because typical convective vertical velocities (say $5m/s$) multiplied by host model time step ($600s$) lead to several thousand meters during each time step. A sub-stepping algorithm may be introduced in the future to reduce this span. An idea of tropical convection precipitation efficiency, as simulated

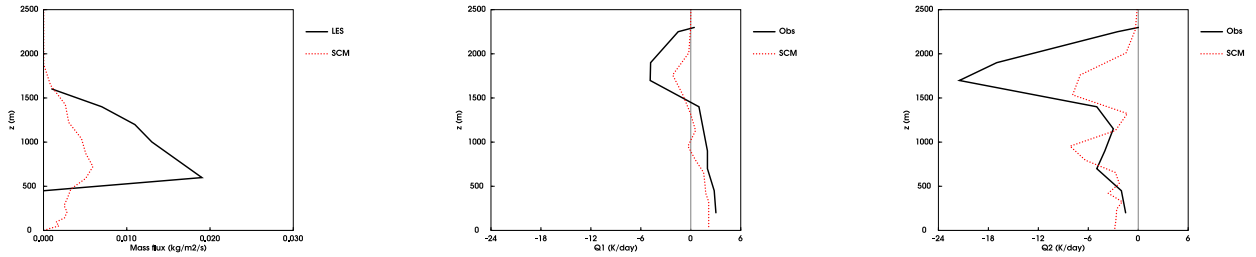

(a) Convective mass flux **(b)** Heat source Q1 **(c)** Moisture sink Q2

Figure 7. BOMEX SCM case. Convective mass flux, heat source Q1 and moisture sink Q2 predicted by the SCM, versus LES reference simulation or observed budget.

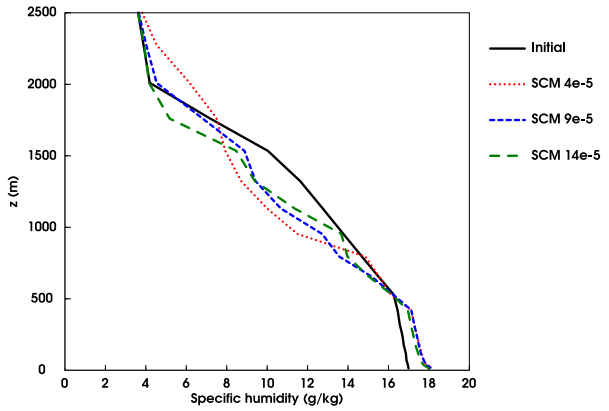

Figure 8. BOMEX SCM case. Initial and final specific humidity profile of the SCM simulation; nominal ϵ_{tx} and $\pm 50\%$.

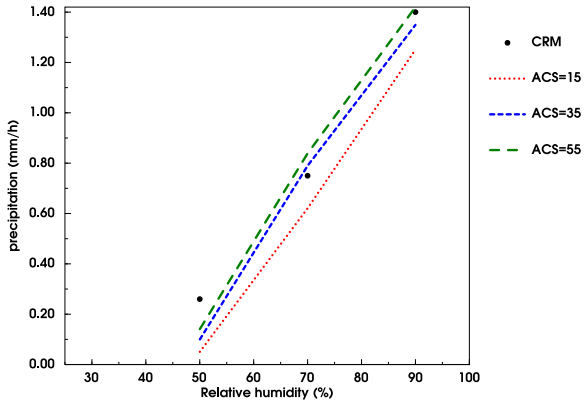

Figure 9. EUROCS SCM idealized humidity case. Mean surface precipitation over the quasi-steady period.

by the present scheme, can be seen in temperature budget Figure 20: a major part of the warming due to latent heat release inside convective drafts (Conv-Microphys) is compensated by the cooling due to evaporation of the detrained liquid, ice, snow and rain in the environment (Env-Microphys).

Figures 21 to 23 show single colum model simulations of the BOMEX case with the PCMT convection scheme, and are to be compared to Figure 3 from Siebesma and Cuijpers (1995). As separating microphysics from transport (equations 2, 15 to 19) the PCMT scheme produces separately the transport term (referred as "turb" on these graphics) and the net condensation term (referred as "c-e" on these graphics). LES do not make difference between convective and turbulent transport, both being resolved; for this reason the process referred as "turb" on these graphics is the sum convection + turbulence. All parameterizations can be validated versus LES using Q1 or Q2 fields, or total temperature tendencies. We can go here a step beyond, in validating separately net condensation and transport versus LES. A useful help in designing convective parameterization schemes.

9. Summary and perspectives

A convection scheme has been developed, PCMT. The guidelines were (i) to increase the sophistication of microphysics, with respect to most current parameterizations, (ii) writing conservative equations of the interaction between convective condensates in the updraft and its environment, closely linked to convective vertical velocity. This opens, from each time step to the next, non-linear feedbacks between entrainment-detrainment processes and condensation-evaporation of cloud condensates and rain/snow. Convective sensitivity to environmental humidity is improved by such feedbacks. Separating microphysics from transport terms makes it possible to call a detailed microphysics scheme, and to validate separately microphysics and transport versus high resolution models, such as CRMs or LES. Perspectives: the downdraft scheme is yet diagnostic, a prognostic one is under development. A specific parameterization of cold pools is also under development, which benefits from evaporative cooling inside microphysics of environmental air, as a source term.

Part II article, in the next pages, shows PCMT 3D GCM results, among which diurnal cycle, precipitation regime, wavenumber-frequency of tropical waves.

References

Bechtold, P., Redelsperger, J.-L., Beau, I., Blackburn, M., Brinkop, S., Grandpeix, J.-Y., Grant, A., Gregory, D., Guichard, F., Hoff, C., and Ioannidou, E. (2000). A gcss model intercomparison for a tropical squall line observed during toga-coare. ii: Intercomparison of single-column models and a cloud-resolving model. *Quart. J. Roy. Meteor. Soc.*, 126:865–888.

Bougeault, P. (1985). A simple parameterization of the large-scale effects of deep cumulus convection. *Mon. Weather Rev.*, 113:2108–2121.

Bouteloup, Y., Seity, Y., and Bazile, E. (2011). Description of the sedimentation scheme used operationally in all Météo-France NWP models. *Tellus A*, 63(2):300–311.

Bretherton, C. S., McCaa, J. R., and Grenier, H. (2004). A new parameterization for shallow cumulus convection and its application to marine subtropical cloud-topped boundary layers. Part I: description and 1D results. *Mon. Weather Rev.*, 132:864–882.

Cuxart, J., Bougeault, P., and Redelsperger, J.-L. (2000). A turbulence scheme allowing for mesoscale and large-eddy simulations. *Quarterly Journal of the Royal Meteorological Society*, 126(562):1–30.

De Hui, C. and Bougeault, P. (1992). A simple prognostic closure assumption to deep convective parameterization: I. *Journal of Meteorological Research*, 7(1):1–18.

Derbyshire, S. H., Beau, I., Bechtold, P., Grandpeix, J.-Y., Piriou, J.-M., Redelsperger, J.-L., and Soares, P. M. M. (2004). Sensitivity of moist convection to environmental humidity. *Quarterly Journal of the Royal Meteorological Society*, 130(604):3055–3079.

Duynkerke, P. G., de Roode, S. R., Zanten, M. C. V., Calvo, J., Cuxart, J., Cheinet, S., Chlond, A., Grenier, H., Jonker, P. J., Khler, M., Lenderink, G., Lewellen, D., Lappen, C.-L., Lock, A. P., Moeng, C.-H., Mller, F., Olmeda, D., Piriou, J.-M., Sanchez, E., and Sednev, I. (2004). Observations and numerical simulations of the diurnal cycle of the eurocs stratocumulus case. *Quart. J. Roy. Meteor. Soc.*, 130(604):3269–3296.

Fowler, L. D. and Randall, D. A. (1996). Liquid and ice cloud microphysics in the CSU general circulation model. Part I, II and III. *Journal of Climate*, 9(3):530–560.

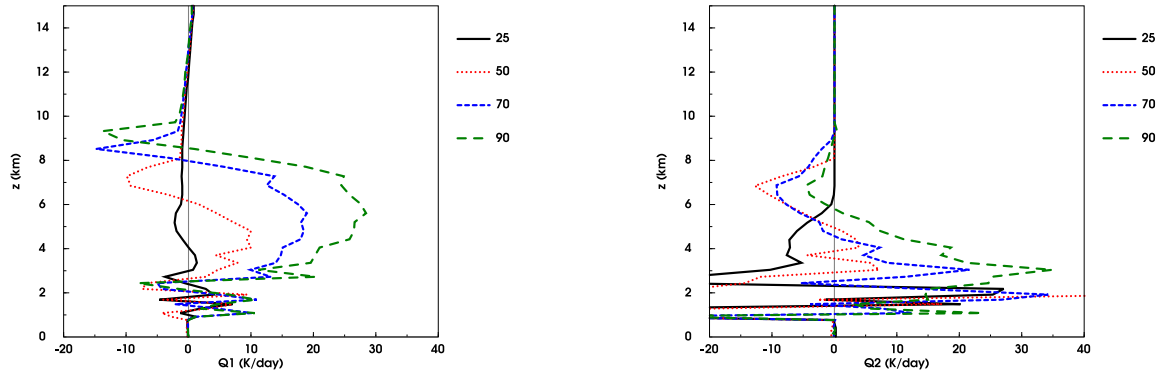

(a) Heat source Q1 **(b)** Moisture sink Q2

Figure 10. EUROCS SCM idealized humidity case. Predicted convective sensitivity to environmental humidity: Q1 and Q2 profiles, for the 4 humidity cases (25, 50, 70 and 90 % respectively).

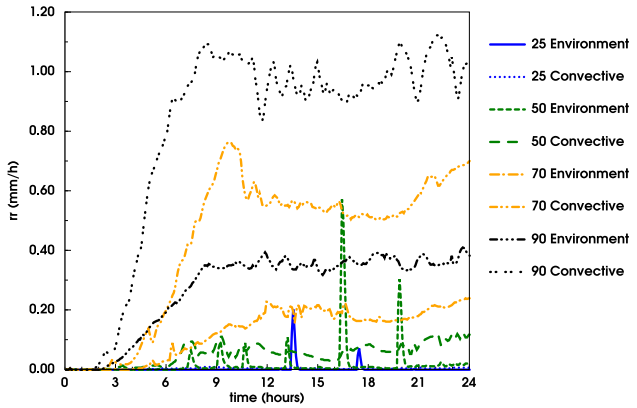

Figure 11. EUROCS SCM idealized humidity case. Precipitation along the 24 hours prediction time, for the 4 humidity cases (25%, 50%, 70% and 90%), separating the two precipitation types from equation 18: convective ($\overline{q_{rc}}$ at surface) and environmental ($\overline{q_{re}}$ at surface).

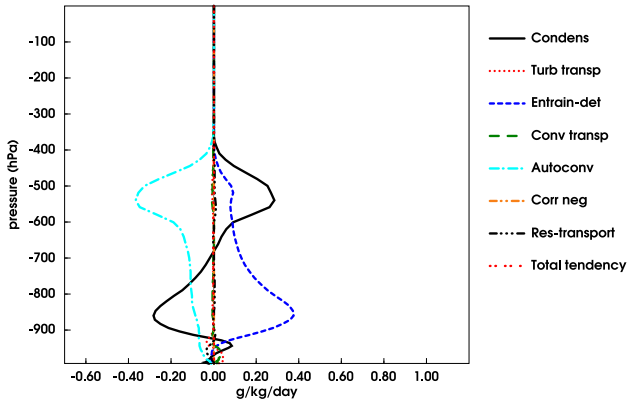

Figure 13. ARPEGE GCM 3 days prediction. Environmental liquid budget q_{le}, equation (15). Turb transport: transport by turbulence (turbulent kinetic energy scheme from Cuxart et al. (2000)); Conv transp: convective transport.

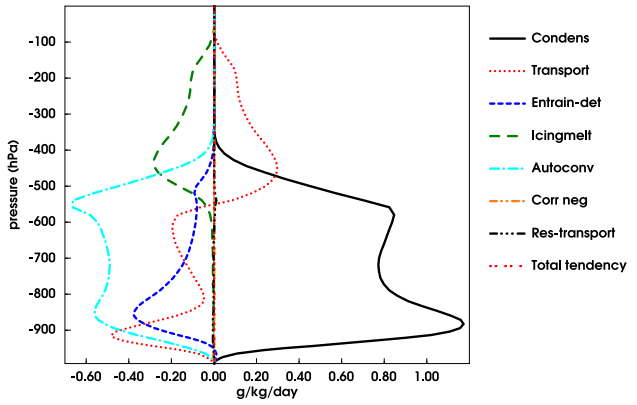

Figure 12. ARPEGE GCM 3 days prediction. Convective liquid budget q_{lc}, equation (15). Condens: condensation; Transport: convective transport; Entrain-det: terms in E and D; Icingmelt: adjustment to local temperature after vertical transport; Autoconv: autoconversion; Corr neg: correct negative values after 3D semi-lagrangian advection; Res-transport: 3D semi-lagrangian advection; Total tendency: mean total tendency during the 3 days simulation.

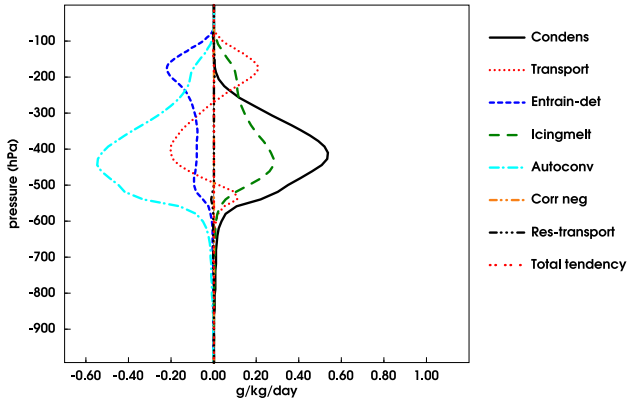

Figure 14. ARPEGE GCM 3 days prediction. Convective ice budget q_{ic}, equation (17).

Geleyn, J.-F., Catry, B., Bouteloup, Y., and Brozkova, R. (2008). A statistical approach for sedimentation inside a microphysical precipitation scheme. *Tellus*, 60(4):649–662.

Guérémy, J.-F. (2011). A continuous buoyancy based convection scheme: one- and three dimensional validation. DOI 10.1111/j.1600-0870.2011.00521.x. *Tellus*, 63A:687–706.

Guichard, F., Petch, J. C., Redelsperger, J.-L., Bechtold, P., Chaboureau, J.-P., Cheinet, S., Grabowski, W., Grenier, H., Jones, C. G., Khler, M., Piriou, J.-M., Tailleux, R., and Tomasini, M. (2004). Modelling the diurnal cycle of deep precipitating convection over land with cloud-resolving models and single-column models. *Quarterly Journal of the Royal Meteorological Society*, 130(604):3139–3172.

Kershaw, R. and Gregory, D. (1997). Parametrization of momentum transport by convection. i: Theory and cloud modelling results. *Quarterly Journal of the Royal Meteorological Society*, 123(541):1133–1151.

Lin, J.-L., Kiladis, G. N., Mapes, B. E., Weickmann, K. M., Sperber, K. R., Lin, W., Wheeler, M. C., Schubert, S. D., Genio, A. D., Donner, L. J., Emori, S., Gueremy, J.-F., Hourdin, F., Rasch, P. J., Roeckner, E., and Scinocca, J. F. (2006). Tropical intraseasonal variability in 14 ipcc ar4 climate models. part i: Convective signals. *Journal of Climate*, 19(12):2665–2690.

Lopez, P. (2002). Implementation and validation of a new prognostic large-scale cloud and precipitation scheme for climate and data-assimilation purposes. *Quarterly Journal of the Royal Meteorological Society*, 128(579):229–257.

Louis (1979). A parameteric model of vertical eddy fluxes in the atmosphere. *Bound.-Lay. Meteorol.*, 17:187–202.

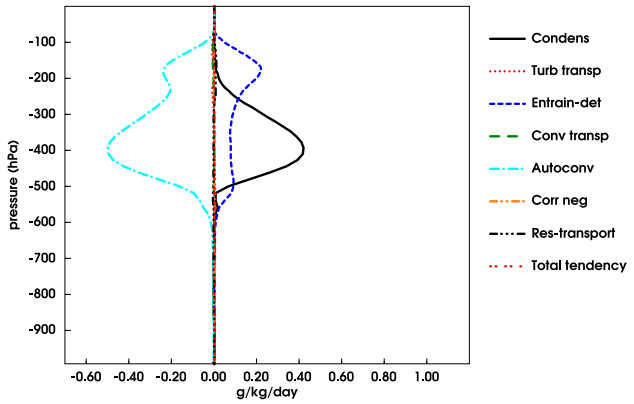

Figure 15. ARPEGE GCM 3 days prediction. Environmental ice budget q_{ie}, equation (17).

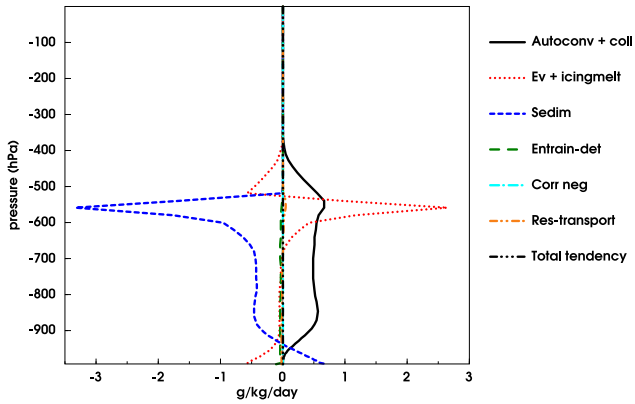

Figure 16. ARPEGE GCM 3 days prediction. Convective rain budget q_{rc}, equation (18). Ev + icingmelt: evaporation + icing-melting; Sedim: sedimentation.

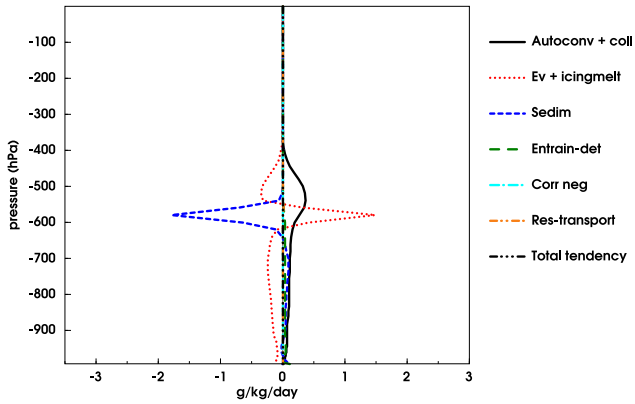

Figure 17. ARPEGE GCM 3 days prediction. Environmental rain budget q_{re}, equation (18).

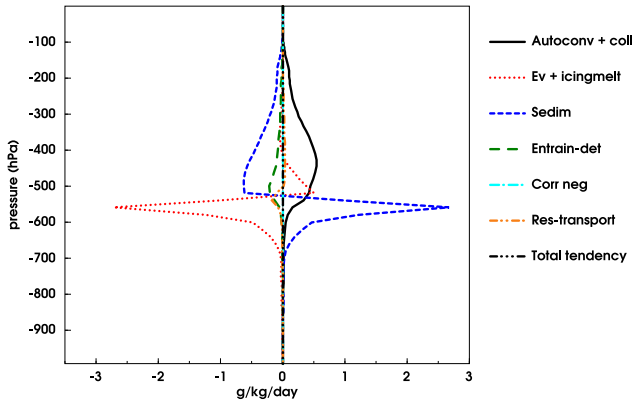

Figure 18. ARPEGE GCM 3 days prediction. Convective snow budget q_{sc}, equation (19).

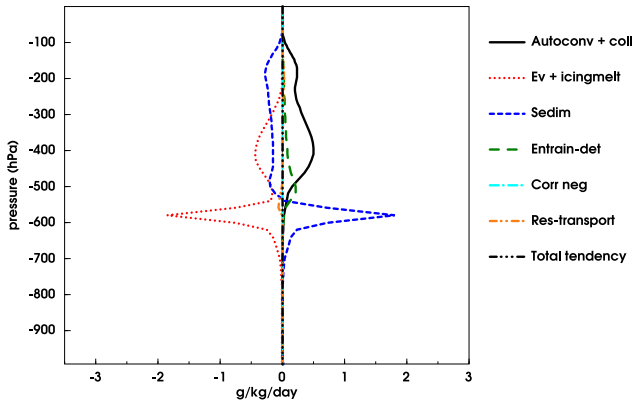

Figure 19. ARPEGE GCM 3 days prediction. Environmental snow budget q_{se} , equation (19).

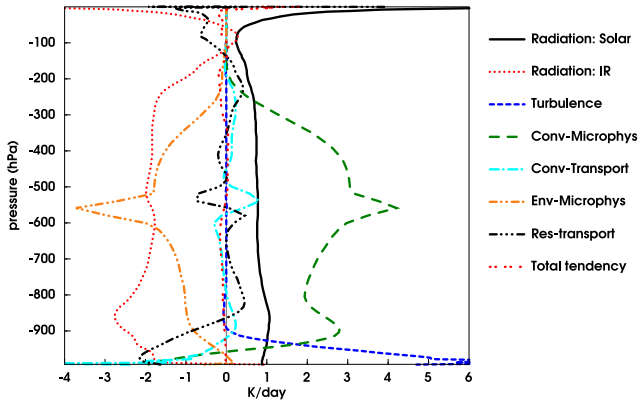

Figure 20. ARPEGE GCM 3 days prediction. Host model temperature budget. Conv-microphys: temperature tendency due to microphysics of convective variables (condensation minus evaporation + icing-melting inside convective cloud); Conv-Transport: convective transport of dry static energy; Env-Microphys: (condensation minus evaporation + icing-melting in convective environment; Res-transport: 3D semi-lagrangian transport of dry static energy.

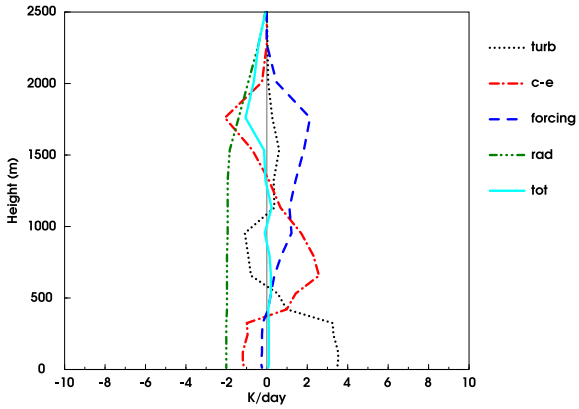

Figure 21. BOMEX SCM case. Temperature budget, mean over the last 16 h. This prediction is to be compared to the LES results Fig. 3 (a) of Siebesma and Cuijpers (1995)

.

Peatman, S. C., Matthews, A. J., and Stevens, D. P. (2015). Propagation of the madden–julian oscillation and scale interaction with the diurnal cycle in a high-resolution gcm. *Climate Dynamics*, 45(9-10):2901–2918.

Piriou, J.-M., Redelsperger, J.-L., Geleyn, J.-F., Lafore, J.-P., and Guichard, F. (2007). An approach for convective parameterization with memory: separating microphysics and transport in grid-scale equations. DOI 10.1175/2007JAS2144.1. *J. Atmos. Sci.*, 64(11):4127–4139.

Rotstayn, L. D. (1997). A physically based scheme for the treatment of stratiform clouds and precipitation in large-scale models. i: Description and evaluation of the microphysical processes. *Quarterly Journal of the Royal Meteorological Society*, 123(541):1227–1282.

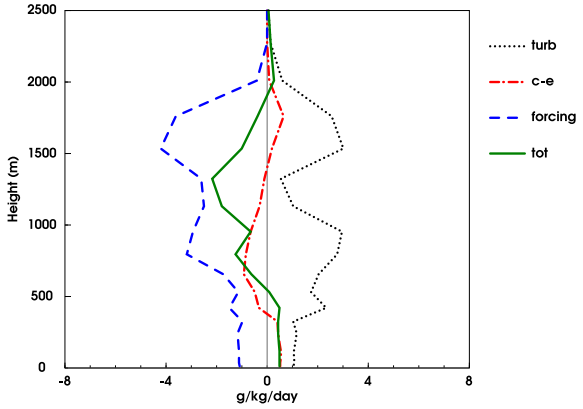

Figure 22. Same as Figure 21, for water vapour budget. To be compared to the LES results Fig. 3 (b) of Siebesma and Cuijpers (1995).

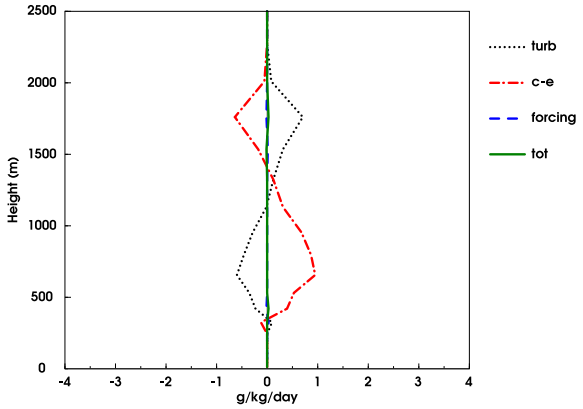

Figure 23. Same as Figure 21, for liquid water budget. To be compared to the LES results Fig. 3 (c) of Siebesma and Cuijpers (1995).

Siebesma, A. P., Bretherton, C. S., Brown, A., Chlond, A., Cuxart, J., Duynkerke, P. G., Jiang, H., Khairoutdinov, M., Lewellen, D., Moeng, C.-H., Sanchez, E., Stevens, B., and Stevens, D. E. (2003). A large eddy simulation intercomparison study of shallow cumulus convection. *J. Atmos. Sci.*, 60:1201–1219.

Siebesma, A. P. and Cuijpers, J. W. M. (1995). Evaluation of parametric assumptions for shallow cumulus convection. *Journal of the Atmospheric Sciences*, 52(6):650–666.

Simpson, J. (1971). On cumulus entrainment and one-dimensional models. *J. Atmos. Sci.*, 28:449–455.

Simpson, J. and Wiggert, V. (1969). Models of precipitating cumulus towers. *Mon. Weather Rev.*, 97:471–489.

Smith, R. (1990). A scheme for predicting layer clouds and their water content in a general circulation model. *Quarterly Journal of the Royal Meteorological Society*, 116(492):435–460.

Tiedtke, M. (1989). A comprehensive mass flux scheme for cumulus parameterization in large-scale models. *Mon. Weather Rev.*, 117:1779–1800.

Turner, J. (1963). The motion of buoyant elements in turbulent surroundings. *Journal of Fluid Mechanics*, 16(1):1–16.

Yano, J.-I., Bister, M., Fuchs, Z., Gerard, L., Phillips, V., Barkidija, S., and Piriou, J.-M. (2013). Phenomenology of convection-parameterization closure. *Atmospheric Chemistry and Physics Discussions*, 13:4111–4131.